

Poly (ethyl 2-cyanoacrylate) nanoparticles (PECA-NPs) as possible agents in tumor treatment

Antonella Obinu^a, Giovanna Rassu^b, Paola Corona^b, Marcello Maestri^c, Federica Riva^d, Dalila Miele^e, Paolo Giunchedi^{b,*}, Elisabetta Gavini^{b,*}

^a Department of Clinical-Surgical, Diagnostic and Paediatric Sciences, University of Pavia, Pavia, Italy

^b Department of Chemistry and Pharmacy, University of Sassari, Sassari, Italy

^c IRCCS Policlinico San Matteo Foundation and Department of Clinical-Surgical, Diagnostic and Paediatric Sciences, University of Pavia, Pavia, Italy

^d Department of Public Health, Experimental and Forensic Medicine-Histology and Embryology Unit, University of Pavia, Pavia, Italy

^e Department of Drug Sciences, University of Pavia, Pavia, Italy

ARTICLE INFO

Keywords:

Tumor treatment

Nanoparticles

Poly (ethyl 2-cyanoacrylate)

Anticancer activity

3D tumor spheroids

ABSTRACT

Tumor eradication has many challenges due to the difficulty of selectively delivering anticancer drugs to malignant cells avoiding contact with healthy tissues/organs. The improvement of antitumor efficacy and the reduction of systemic side effects can be achieved using drug loaded nanoparticles. In this study, poly (ethyl 2-cyanoacrylate) nanoparticles (PECA-NPs) were prepared using an emulsion polymerization method and their potential for cancer treatment was investigated. The size, polydispersity index and zeta potential of prepared nanoparticles are about 80 nm, 0.08 and -39.7 mV, respectively. The stability test shows that the formulation is stable for 15 days, while an increase in particle size occurs after 30 days. TEM reveals the spherical morphology of nanoparticles; furthermore, FTIR and ^1H NMR analyses confirm the structure of PECA-NPs and the complete polymerization. The nanoparticles demonstrate an *in vitro* concentration-dependent cytotoxicity against human epithelial colorectal adenocarcinoma cell lines (Caco-2), as assessed by MTT assay. The anticancer activity of PECA-NPs was studied on 3D tumor spheroids models of hepatocellular carcinoma (HepG2) and kidney adenocarcinoma cells (A498) to better understand how the nanoparticles could interact with a complex structure such as a tumor. The results confirm the antitumor activity of PECA-NPs. Therefore, these systems can be considered good candidates in tumor treatment.

1. Introduction

Cancer is one of the deadliest diseases in the world and it is the first cause of death in developed countries [1]. Conventional therapeutic strategies include surgery, chemotherapy and radiotherapy [2]; however, cancer treatments present several disadvantages such as heavy side effects, resistance to anti-cancer agents, relapses and metastatic phenomena. All these problems represent a challenge for new anticancer therapies. The main goal of tumor treatment is to achieve therapeutic drug concentration in target tumor tissues, avoiding side effects towards healthy tissues [3].

Nano-drug delivery systems can improve the equilibrium between the efficacy and the toxicity of active agents, by delivering chemotherapeutic drugs more selectively to cancer sites (site-specific drug delivery). Over the years, different concepts have been proposed for nanomedicine-mediated drug targeting, including passive drug

targeting and active targeting to cancer cells [4]. The small size of nano-drug delivery systems enables them to exploit the unique anatomical–pathophysiological nature of solid tumors, which are characterized by poorly differentiated and tortuous blood vessels that are suitable for the extravasation of particles with sizes of up to several hundreds of nanometers. In addition, solid tumors lack of functional lymphatic vessels and thus are not able to eliminate extravasated nano-drug delivery systems that, consequently, accumulate in tumors over the time [5]. This phenomenon is called “Enhanced Permeability and Retention (EPR) effect” and is the principal mechanism of passive drug targeting in tumor treatment [6]. Conversely, the goal of active drug targeting is to improve selective cellular uptake and recognition; hence, it is based on the use of targeting ligands as peptides and antibodies that can interact with receptors expressed at the target site [7,8]. Therefore, new anti-cancer therapies based on nanotechnology have been developed with the aim of overcoming drug resistance and increasing the

* Corresponding authors at: Department of Chemistry and Pharmacy, University of Sassari, via Muroni 23a, 07100 Sassari, Italy.

E-mail addresses: pgiunc@uniss.it (P. Giunchedi), eligav@uniss.it (E. Gavini).

<https://doi.org/10.1016/j.colsurfb.2019.02.036>

Received 17 October 2018; Received in revised form 29 January 2019; Accepted 19 February 2019

Available online 19 February 2019

0927-7765/ © 2019 Elsevier B.V. All rights reserved.

specificity and selectivity of therapeutic agents against cancer cells [9,10]. Examples of nanomedicine formulations for the treatment of solid tumors include liposomes, micelles, polymers, nanoparticles (NPs), antibodies and many more systems that are in preclinical or clinical trials [11]. Some peculiarities such as size, charge, surface characteristics, biocompatibility and controlled degradation make the NPs suitable drug delivery systems for transport and release of anti-cancer agents in malignant cells [12]. Several reports suggest that by loading chemotherapeutics into NPs, the more advantageous biodistribution and pharmacokinetics can improve the efficacy of drugs. For example, Pan et al. showed that, when compared with free doxorubicin, pH-sensitive poly (β -thiopropionate) NPs had the strongest cytotoxicity against breast cancer cells [13], whereas Rychahou et al. demonstrated that polymeric NPs provide a new therapeutic strategy for treating colorectal cancer lung metastasis [14]. Quinto et al. prepared supermagnetic iron oxide NPs loaded with doxorubicin and they found that the merged effect of NPs and doxorubicin induced-hyperthermia enhanced cancer cell death *in vitro* [15]. Currently, among several NPs developed for possible use in cancer treatment, polymeric NPs represent promising drug delivery systems, mainly because of their well-known features of biocompatibility, easy preparation and functionalization, sustained drug release and the possibility to control degradation rate [16].

Poly (ethyl 2-cyanoacrylate) (PECA) was used for NP preparation. This polymer belongs to the family of poly (alkyl cyanoacrylates) which, are extensively used like adhesive polymers in surgery, for joining tissues and like hemostatic substances [17,18]. Interesting characteristics such as biodegradability, drug compatibility and biocompatibility, make these polymers suitable for the preparation of injectable nanoparticulate drug delivery systems [19,20]. To date, the use of poly (alkyl cyanoacrylates) as a component of nano-drug delivery systems has been reported in several works [21–23]. One of the most interesting applications of NPs based on poly (alkyl cyanoacrylates) is their use in cancer treatment [24]. This therapeutic activity can be attributed to the combination of different factors: (a) the cytotoxicity induced by therapeutic agents entrapped into the nano-drug delivery systems; (b) the toxic effects induced by high concentration of polymeric degradation products at the cell membrane that can allow cellular death or inhibition of cell growth; (c) the reduction of the drug resistance due to the adhesion of drug-loaded NPs on the cell surface [25].

In this study, PECA-NPs were prepared in order to improve the eradication of malignant cells. The best formulation conditions were investigated and, after preparation, the physical and chemical properties of NPs were assessed. Furthermore, the MTT assay was used to evaluate the cytotoxicity of the formulation on Caco-2 cell line.

Despite many authors suggest the use of poly (alkyl cyanoacrylates) NPs in tumor treatment [26,27], the assessment of anticancer properties of these NPs on three-dimensional (3D) multicellular spheroid models is not reported. Generally, monolayer cell culture in two dimensions is the main method of cultivation of cells in laboratories and to date is the most common technique used for the assessment of therapeutics effects of anticancer drugs. However, two-dimensional cell cultures do not represent the physiology and anatomy of tissue; therefore, the various transport conditions and the specific cell-matrix and cell-cell interactions are not present. Models for the evaluation of cytotoxicity need to reproduce the *in vivo* situation as closely as possible. Compared to traditional cell cultures, multicellular spheroids better mimic real solid tumors; hence they are suitable models to predict the *in vivo* behavior of the drug delivery systems [28]. Tumor spheroids are used to evaluate drug resistance and sensitivity; in addition, they develop regions of hypoxia and necrosis, characteristic of several cancers, which are critical for studying chemotherapeutic agents. Interestingly, multicellular spheroids show greater chemoresistance when compared with monolayer cell cultures [29,30]. Then, in order to better predict the *in vivo* antitumor activity of PECA-NPs, a toxicity study was

conducted on 3D tumor spheroid models of hepatocellular carcinoma cells and kidney adenocarcinoma cells.

2. Materials and methods

2.1. Materials and reagents

Ethyl 2-cyanoacrylate (ECA) used as a monomer for the polymerization and Tween 20 were obtained from Sigma-Aldrich (St. Louis, USA). Phosphotungstic acid was purchased from Carlo Erba reagents s.r.l. (Milan, Italy). Antibiotic/antimycotic solution (100 \times), containing 10,000 units/ml penicillin, 10 mg/ml streptomycin and 25 mg/ml amphotericin B and dimethyl sulfoxide (DMSO) were purchased from Sigma-Aldrich (Milan, I); Dulbecco's Modified Eagles Medium (DMEM, with 4.5 g/l glucose, L-glutamine and sodium pyruvate) was purchased from Corning (Mediatech Inc. A Corning Subsidiary Manassas, USA); Dulbecco's Phosphate Buffer Solution and inactivated foetal bovine serum were acquired from Biowest (Nuaille, F); MTT (3-(4,5-dimethylthiazol-2-yl)-2,5-diphenyltetrazolium bromide) and trypan blue solution were purchased from Sigma-Aldrich (Milan, I). Cell-line culture Caco-2 was obtained from European Tissue Culture Collection. HepG2 and A498 cell lines were obtained from the ICLC (Interlab Cell Line Collection, Genoa, Italy). CellTox green cytotoxicity assay kit was purchased from Promega (Madison, WI, USA). Ultrapure bi-distilled water was obtained by a MilliQ R4 system, Millipore (Milan, Italy). All other chemicals and reagents were of analytical grade.

2.2. Caco-2, Caucasian colorectal adenocarcinoma from human colon

Cells were cultured in a polystyrene flask (Greiner bio-one, PBI International, Milan, Italy) with 12 ml of complete culture medium (CM) consisting of DMEM with 4.5 g/l glucose and L-glutamine supplemented with 1% (v/v) antibiotic/antimycotic solution and 10% (v/v) inactivated foetal bovine serum. Cells were kept in an incubator (Shellab[®] Sheldon[®] Manufacturing Inc., Oregon, USA) at 37 °C with 95% air and 5% CO₂ atmosphere. After cells reached 80–90% confluence, trypsinization was performed. The cell monolayer was washed with Dulbecco's Phosphate Buffer Solution (PBS) and then 3 ml of 0.25% (w/v) trypsin-EDTA solution was left in contact with cell for 5 min. After that time, the cell layer was harvested with 7 ml of the CM to stop the proteolytic activity of trypsin and to facilitate the detachment of cells. Afterward, cell suspension was centrifuged (TC6, Sorvall Products, Newtown, USA) at 1200 rpm for 10 min and then cells pellet was re-suspended in 6 ml of CM. The number of cells in suspension was determined in a counting chamber (Hycor Biomedical, Garden Grove, California, USA), using 0.5% (w/v) trypan blue solution to visualize and count viable cells.

2.3. Preparation of PECA-NPs

PECA-NPs were prepared using an emulsion polymerization method, partially modified [31,32]. The influence of the following parameters on the particle size, dispersion homogeneity and polymerization rate was studied: (a) concentration of monomer; (b) concentration of surfactant.

Briefly, the non-ionic surfactant Tween 20 (0.5% w/v) was dissolved in 10 ml of an aqueous solution of hydrochloric acid (pH 2.5) to prepare the polymerization medium. Then, three different volumes of ECA (200, 100 and 50 μ l) were dripped into the medium, under continuous magnetic stirring at room temperature, to obtain the final monomer concentrations of 2.0, 1.0 and 0.5% (w/v) (formulations PECA-NPs 1-3). The mechanical stirring was maintained until the polymerization was complete (commonly 3 h). After polymerization, the NP dispersion was neutralized at pH 7.4 by the addition of 0.2 M NaOH, to ensure the end of the reaction. In order to remove all the reagents in excess, an ultrafiltration procedure on Amicon[®] devices

Table 1
Composition and preparation techniques of all the formulations prepared.

Sample	ECA monomer (v/v)	Tween 20 (w/v)	Magnetic stirring	Ultra Turrax	Probe sonicator
PECA-NPs 1	2.0%	0.5%	✓		
PECA-NPs 2	1.0%	0.5%	✓		
PECA-NPs 3	0.5%	0.5%	✓		
PECA-NPs 4	2.0%	1.0%	✓		
PECA-NPs 5	1.0%	1.0%	✓		
PECA-NPs 6	0.5%	1.0%	✓		
PECA-NPs 7	1.0%	1.0%		✓	
PECA-NPs 8	1.0%	1.0%			✓

30,000 Da MWCO was used. The suspension volume was firstly concentrated to 1 ml and then, 10 ml of bi-distilled water were added and the ultrafiltration was carried out. This purification procedure was repeated several times. The influence of the surfactant concentration was evaluated. An acidic solution containing an increased concentration of Tween 20 (1.0% w/v) was prepared and the different concentrations of ECA (2.0, 1.0 and 0.5% v/v) were dripped into this medium with the method previously described to obtain the samples PECA-NPs 4-6.

Once the ideal composition of NPs was identified, the influence of the process parameters on the NPs formation was evaluated by testing two different techniques for the dispersion of the monomer in the medium. They were: homogenization with Ultra Turrax T-25 digital (IKA, Staufen, Germany) at 8600 rpm for 5, 10, 15 and 30 min (PECA-NPs 7) and sonication using a probe sonicator Vibra Cell, VC 50 (Sonics and Materials, Danbury, USA) at 50 W for different times (1, 2, 4, 6, and 10 min) (PECA-NPs 8). Table 1 summarizes the composition and the preparation techniques of all the suspensions prepared.

On the basis of these preliminary studies, the leader formulation was select and further studies were performed as described below.

2.4. Physicochemical characterization of PECA-NPs

2.4.1. Dimensional analysis

Particle size and PDI (polydispersity index) were determined by a dynamic light scattering method using a Coulter Submicron Particle Sizer N5 (Beckman-Coulter Inc. Miami, Florida, USA).

All the studies reported below were performed only on the formulation selected as leader.

2.4.2. Physical stability and zeta potential

The NPs were stored both at 25 °C and at 4 °C and their physical stability as a function of the time and storing conditions was assessed. The homogeneity of the colloidal suspensions was observed macroscopically; furthermore, the NPs were analyzed in terms of mean diameter and PDI during the time (7, 15 and 30 days). The results were compared with those obtained at the time of preparation to evaluate if any variations occur over time. In addition, the colloidal stability of the NPs was evaluated in fetal bovine serum (FBS). For this purpose, 2 ml of NPs were dispersed into an appropriate volume of FBS. The dispersion was stored at 4 °C and the NP stability during the time (within 15 days) was evaluated as above reported. The formulation stability was not assessed at 25 °C due to the instability of serum at room temperature.

Zeta-potential of leader formulation was measured in water at 25 °C and at a conductivity of 0,019 mS/cm, using a Litesizer 500 (Anton Paar, Austria).

2.4.3. Morphological observations

To describe the morphological characteristics of PECA-NPs, an ultrastructural approach by transmission electron microscopy (TEM) was used. At the first, NP formulations in aqueous suspension were investigated, dropping 15 µl of the concentrated suspension on 200 mesh

Formvar Carbon-coated copper grids (FCF200-Cu, Electron Microscopy Sciences, Fort Washington, PA, USA). After 15 min, samples were gently dried with whatman paper (Whatman® Cellulose Filter Paper – Sigma-Aldrich) and 10 µl of 1% Phosphotungstic Acid solution (Carlo Erba, Milan, Italy) was added on the F/C coated grids for 30 s. In order to prevent artifacts, particular care has been taken for proper drying, quickly touching the grid edge with whatman paper and finally storing the grids overnight at room temperature. Then, specimen grids were put in the vacuum column of the electron microscope and the negatively stained preparations were examined at the electron microscope [33]. TEM observations were carried out on a JEOL JEM-1200 EX II microscope operating at 100 kV (tungsten filament gun) and equipped with the TEM CCD camera Olympus Mega View III at different magnifications in the range 12,000×–100,000×. TEM calibration was made on lattice plane spacings of standard negatively stained Catalase Crystals (Agar scientific, Stansted, UK).

NPs measurements were made directly on the original images by means of ImageJ software [34] at the same high magnification for all samples.

2.4.4. FTIR and ¹H NMR analysis

Structural characterization of PECA-NPs was evaluated by Fourier transform infrared spectrometry (FTIR) and proton nuclear magnetic resonance (¹H NMR) analyses. For that purpose, NPs were washed and concentrated with Amicon® devices and the resulting dispersion was freeze-dried at –54.5 °C under vacuum (0.909 mbar) for 8 h with a Lio 5P (Cinquepascal Trezzano sul Naviglio, Italy) to obtain white powder material. FTIR spectra were obtained with a Nicolet Avatar 320 FTIR spectrometer (Nicolet Instrument Corporation, Madison, WI, USA) preparing the samples with the KBr-tablet technique. ¹H NMR spectrum was determined in DMSO-*d*₆ and was recorded with a Bruker Avance III 400 NanoBay. Chemical shifts are reported in parts per million (ppm) downfield from tetramethylsilane (TMS) used as internal standard.

2.5. Cytotoxicity assay

The effect of different concentrations of PECA-NPs on the viability of human colorectal adenocarcinoma cells (Caco-2) was investigated by MTT assay. Cells were seeded on 96-well plates (2.0 × 10⁴ cells in 200 µl of CM/well) and incubate (37 °C and 5% CO₂) for 24 h to reach semi-confluence. The samples were prepared in sterile bidistilled water and were diluted (750, 75 and 7.5 µg/ml) in CM and 200 µl of each sample were put in contact for 24 h with cells; CM was used as a reference. After 24 h contact with samples, an MTT assay was performed. Cells were washed with 100 µl of PBS (pH 7.4) and then put in contact for 3 h (37 °C and 5% CO₂) with 50 µl of MTT 7.5 µM in 100 µl of DMEM without phenol red. Finally, 100 ml of DMSO was added to each well, to allow the complete dissolution of formazan crystals, obtained from MTT dye reduction by mitochondrial dehydrogenases of live cells. After 60 shakings, the solution absorbance was determined at 570 nm, with a 690 nm reference wavelength, by means of an IMark1 Microplate reader (Bio-Rad Laboratories S.r.l., Segrate, Milan, I). Results were expressed as % cell viability calculated by normalizing the absorbance measured after contact with samples with that measured after contact with pure CM, used as positive control. Eight replicates were performed for each sample.

2.6. Antitumor activity of PECA-NPs in 3D tumor spheroid models

Antitumor activity of PECA-NPs was evaluated *in vitro* in two different 3D tumor spheroid models. Hepatocellular carcinoma cells (HepG2) and kidney adenocarcinoma cells (A498) were seeded into 384 multi-well ultra-low attachment (ULA) transparent-bottom black plates (Corning, NY, USA). In these plates, wells are U-bottom and coated with a synthetic hydrogel to favor the formation of a single spheroid in each well [35]. Spheroid death was evaluated by the addition of CellTox

green dye (Promega) to the culture medium [36]. Briefly, 500 cells were plated in each well in a volume of 20 μ l; after three days to let the formation of spheroids, eight 1:2 serial dilutions of NPs ranging from 375 to 2.9 μ g/ml were added to culture medium together with CellTox 0.33 \times in a final volume of 30 μ l. Immediately after the start of treatment, spheroids were incubated at 37 °C and 5% CO₂ in BioTek Cytation 5 (Bio-Tek Instruments, Winooski, VT). Live-cell images were collected after 15 min and at 6, 12, 18 and 24 h after treatment. After 24 h, plates were moved to a standard incubator at 37 °C and 5% CO₂ and live-cell images were collected at 48 and 72 h after treatment. Spheroid area (A) and green fluorescence intensity (GFI), limited to spheroid area, were calculated using Gen5 software. (A) was used to calculate spheroid volume (V): $4/3 \times A \times \text{RADQ}(A/\pi)$ [37]. Spheroid volume is calculated as V/V_0 , where V is spheroid volume at each time point and V₀ is the volume of the same spheroid 15 min after compound addition. Spheroid death was calculated as $(\text{GFI}-\text{GFI}_0)/A$, where GFI is green fluorescence intensity at each time point and GFI₀ is green fluorescence intensity 15 min after compound addition.

2.7. Statistical analysis

Data were analyzed using analysis of variance (ANOVA). Individual differences between data were identified using non-parametric Tukey's post-hoc tests. Values are expressed as mean \pm standard deviation (SD). $P < 0.05$ was considered statistically significant (GraphPad Instat Software Program, GraphPad Software Inc, San Diego, CA, USA).

3. Results

3.1. Preparation of PECA-NPs

NPs were prepared with an emulsion polymerization method with Tween 20 as a surfactant.

Using 0.5, 1.0 or 2.0% (w/v) of monomer, significant differences in the NP dispersions were obtained. With concentration of 2% (PECA-NPs 1 and PECA-NPs 4) clearly visible aggregates were observed, while when the ECA concentration was decreased from 2% to 0.5% (PECA-NPs 3 and PECA-NPs 6) a very clear dispersion was obtained, which indicated a slow polymerization rate and a reduced concentration of NPs. The formulations with monomer concentration of 1% were morphologically different: the sample PECA-NPs 2 was characterized by several aggregates, conversely the formulation PECA-NPs 5 appeared homogeneous and milky white, without aggregates. This difference was probably due to the different concentrations of Tween 20 used.

The results of the studies performed varying the concentration of Tween 20 showed that the best surfactant concentration was 1.0% (w/v). Tween 20 concentration below 1.0% was unsuitable for the preparation of stable NPs. In all the formulations prepared with a concentration of Tween 20 of 0.5% (PECA-NPs 1-3), aggregates of NPs were observed. The results of dimensional analysis of formulations PECA-NPs 4-6 (prepared with 1.0% of Tween 20 and different concentrations of ECA) showed that the particle size increased with decreasing monomer concentration ($P < 0.05$). The values of PDI increased significantly when the monomer concentration decreased from 2.0 to 1.0 and 0.5% ($P < 0.05$), while no obvious change in PDI occurred when the ECA concentration decreased from 1.0 to 0.5% ($P > 0.05$) (Table 2). On the basis of these results, the best composition of NPs was identified: 1.0% (v/v) of ECA and 1.0% (w/v) of Tween 20.

Afterward, alternative techniques to disperse the monomer into the polymerization medium were investigated. The Ultra Turrax was found to be unsuitable due to the formation of several aggregates during the polymerization reaction. Moreover, from Table SI 1 it can be seen that the particle size and the PDI of formulations exhibited an increase prolonging the homogenization time ($P < 0.05$). The use of the ultrasonic probe revealed that the particle size did not increase within the first four minutes of sonication ($P > 0.05$), whereas prolonging the

Table 2

Particle size and PDI of formulations containing 1.0% (w/v) of Tween 20 and 2.0, 1.0 and 0.5% (w/v) of ECA monomer. $P < 0.05$: * PECA-NPs 4 vs PECA-NPs 5 and PECA-NPs 6; § PECA-NPs 5 vs PECA-NPs 6; # PECA-NPs 4 vs PECA-NPs 5 and PECA-NPs 6.

Sample	Mean diameter (nm)	PDI
PECA-NPs 4	60 \pm 0.03*	0.06 \pm 0.003#
PECA-NPs 5	80 \pm 0.04*§	0.08 \pm 0.03#
PECA-NPs 6	108.1 \pm 0.01*§	0.08 \pm 0.001#

sonication time led to NPs aggregation ($P < 0.05$). Furthermore, the suspension homogeneity was reduced when the sonication time was increased ($P < 0.05$) (Fig. SI 1). Consequently, Ultra Turrax and sonication can be considered unsuitable techniques for NP preparation. In contrast, a homogeneous dispersion and acceptable size were obtained dispersing the monomer with a magnetic stirring for 3 h (mean diameter 80 \pm 0.04 nm and PDI 0.8 \pm 0.03). On the basis of these preliminary results the formulation PECA NPs 5 was selected as a leader formulation for the further studies reported below.

3.2. Physicochemical characterization of PECA-NPs

3.2.1. Dimensional analysis

The mean diameter for PECA-NPs 5 as determined by dynamic light scattering was found to be 80 \pm 0.04 nm with a PDI of 0.08 \pm 0.03, indicating the uniformity of the particle size distribution.

3.2.2. Physical stability and zeta potential

Fig. 1 reports the stability trends of NPs in terms of particle size and PDI within the time, as a function of the storage conditions. The dimensional analysis showed that the NPs were stable for 15 days ($P > 0.05$), although an increase in particle size occurred after 30 days ($P < 0.05$), both at 25 °C and 4 °C. In terms of PDI, no significant changes occurred over the time ($P > 0.05$), indicating a good homogeneity of NP dispersion. Furthermore, there were no visible aggregates of particles.

The colloidal stability of the NPs was also evaluated in FBS (Fig. SI 2) and an increase in particle size and PDI (102.8 \pm 2.76 and 0.252 \pm 0.02 respectively) was observed when NPs were dispersed in serum. The results showed that the particle size increased during the first 10 days ($P < 0.05$), while neither variation occurred after this time ($P > 0.05$). On the contrary, PDI values of PECA-NPs 5 were not modified over time ($P > 0.05$).

The zeta potential of PECA-NPs 5, measured in water, was negative (-39.7 ± 2.45 mV).

3.2.3. Morphological observations

Transmission Electron Microscopy analysis was performed on negatively stained specimens using carbon-coated grids as support to better identify the NPs (Fig. 2). PECA-NPs appeared as isolated, rounded in shape particles (Fig. 2A 12,000 \times), and in order to better investigate their structure, subsequent observations were conducted at a higher magnification (100,000 \times). Inside them, two different types of small granules were identified, some electrontransparent, others electron-dense (Fig. 2B). These structures appeared clearly due to the penetration inside NPs of the dark phosphotungstic acid used in the negative staining procedure for ultrastructural preparation and also maybe due to the bubble generation during PECA-NPs synthesis process, as reported by Matsubayashi et al. [38].

3.2.4. FTIR and ¹H NMR analysis

Characterization of NPs by FTIR and ¹H NMR spectroscopies confirmed the composition and the chemical structure of the polymer. The FTIR spectrum of PECA-NPs 5 (Fig. SI 3) revealed the characteristic

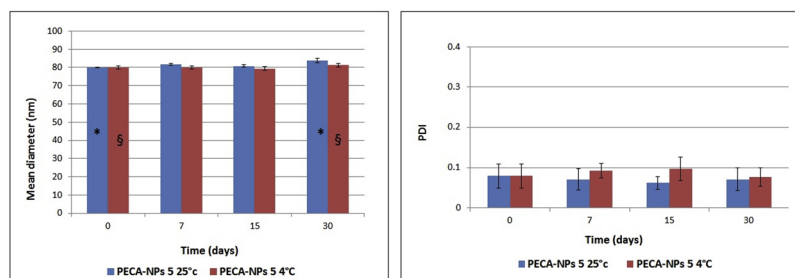


Fig. 1. Physical stability of PECA-NPs 5 in terms of particle size and PDI during the time. $P < 0.05$: * PECA-NPs 5 25 °C 0 days vs PECA-NPs 5 25 °C 30 days; § PECA-NPs 5 4 °C 0 days vs PECA-NPs 5 4 °C 30 days.

absorption bands for carbonyl $C=O$ ester (1750 cm^{-1}), CN (2250 cm^{-1}) and C–O stretching (1254 cm^{-1}). The peaks at around $3000\text{--}2880\text{ cm}^{-1}$ were from symmetric and asymmetric –CH stretching vibrations of methylene and methyl groups in the ethyl substituent. The ^1H NMR spectrum is shown in Fig. SI 4. The broad singlet at δ 1.24–1.31 ppm was due to methyl groups of ethyl ester, the multiplet at δ 2.51–2.85 ppm was ascribed to the methylene group in the backbone of the chain, the triplet at δ 4.12 was the terminal –CH of the chain and finally the multiplet at δ 4.13–4.22 ppm was due to the protons of methylene of ethyl ester groups. The absence of the peaks of the olefinic protons at δ 6.65 and δ 7.07 ppm indicated that there was no unpolymerized monomer.

3.3. Cytotoxicity assay

The cytotoxicity of PECA-NPs 5 was evaluated on Caco-2 cells after 24 h incubation *via* MTT assay. The effects of decreasing NPs concentration from 750 to 7.5 $\mu\text{g/ml}$ on Caco-2 viability are shown in Fig. 3. The results revealed that PECA-NPs 5 suppressed cell proliferation dose-dependently. No cytotoxicity was observed at a NPs concentration of 7.5 $\mu\text{g/ml}$, while the cell viability was about 4% when the concentration of NPs increased to 75 and 750 $\mu\text{g/ml}$.

3.4. Antitumor activity of PECA-NPs in 3D tumor spheroid models

Cytotoxicity of PECA-NPs 5 was tested in 3D tumor spheroid models of HepG2 and A498 cells. As reported by Lankoff et al., the most important challenge in nanotoxicology was the stability of NPs in several aqueous suspensions [39]. Therefore, as a preliminary experiment, precipitation of the formulation in the complete cell culture medium was examined. No clustered NPs were observed, suggesting that the system was stable in the medium (data not shown). As shown in Figs. 4 and 5, the treatment with NPs induced significant death in both tumor models, albeit a significant increase in cell death was observed in HepG2 spheroids at a lower concentration compared to A498 spheroids (12 $\mu\text{g/ml}$ in A498, 5.9 $\mu\text{g/ml}$ in HepG2). Cell death was detected after 6 h of treatment and it was maintained for the entire time course

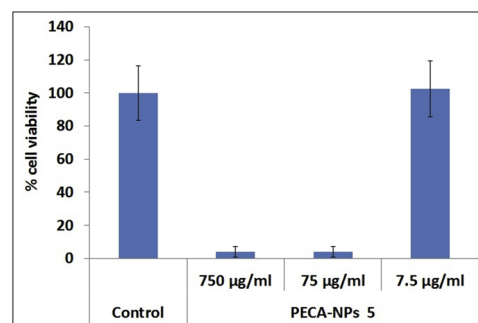


Fig. 3. MTT test of PECA-NPs 5 against Caco-2 cells.

(Fig. 5). Furthermore, shatter of spheroid morphology was observed after 6 h of treatment in both models at higher concentrations of NPs, indicating rapid massive cell death (Fig. 4, 47 $\mu\text{g/ml}$ or higher in both tumor models). Subsequently, analysis of tumor growth was carried out at NP concentrations where shatter of spheroids was not observed. As shown in Fig. 6, increased cell death was accompanied by growth reduction in HepG2 spheroids up to 5.9 $\mu\text{g/ml}$ NP concentration. In A498 cells, it is likely that growth reduction was not observed in treated samples since tumor growth was observed neither in untreated spheroids. Neither growth reduction nor cell death were observed in both spheroid models treated with NPs at 2.9 $\mu\text{g/ml}$ concentration. In both models, treatment efficacy was improved with the increasing of NP concentration and extending of exposure time.

4. Discussion

The polymerization of poly (alkyl cyanoacrylates) in aqueous solution proceeds *via* an anionic mechanism and it is initiated by the bases existent into the polymerization medium [40,19]. The presence of two powerful electron-withdrawing groups in the α -carbon of the double bond (–COOR and –CN) of alkyl cyanoacrylate structure, makes these monomers very reactive against nucleophiles like bases and anions [41]. Therefore, weak bases such as OH^- can ionize the monomer

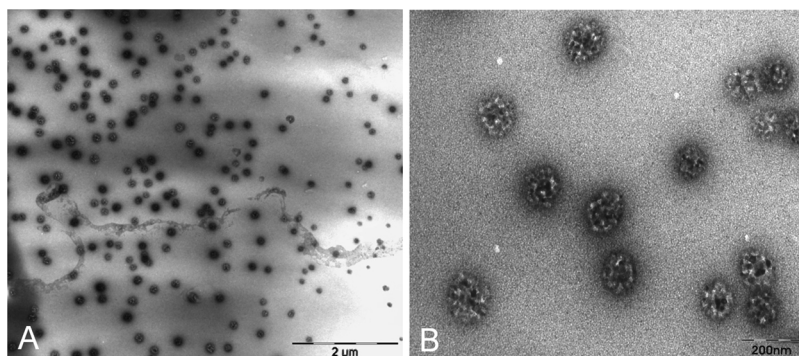


Fig. 2. Ultrastructural morphology of negatively stained PECA-NPs (PECA-NPs 5). A) PECA-NPs 5 appeared singularly dispersed on the supporting surface at magnification of 12,000 \times (scale bar: 2 μm). B) At the higher magnification 100,000 \times (scale bar: 200 nm) single NPs appeared rounded and similar for dimension. Negative staining revealed an internal substructure.

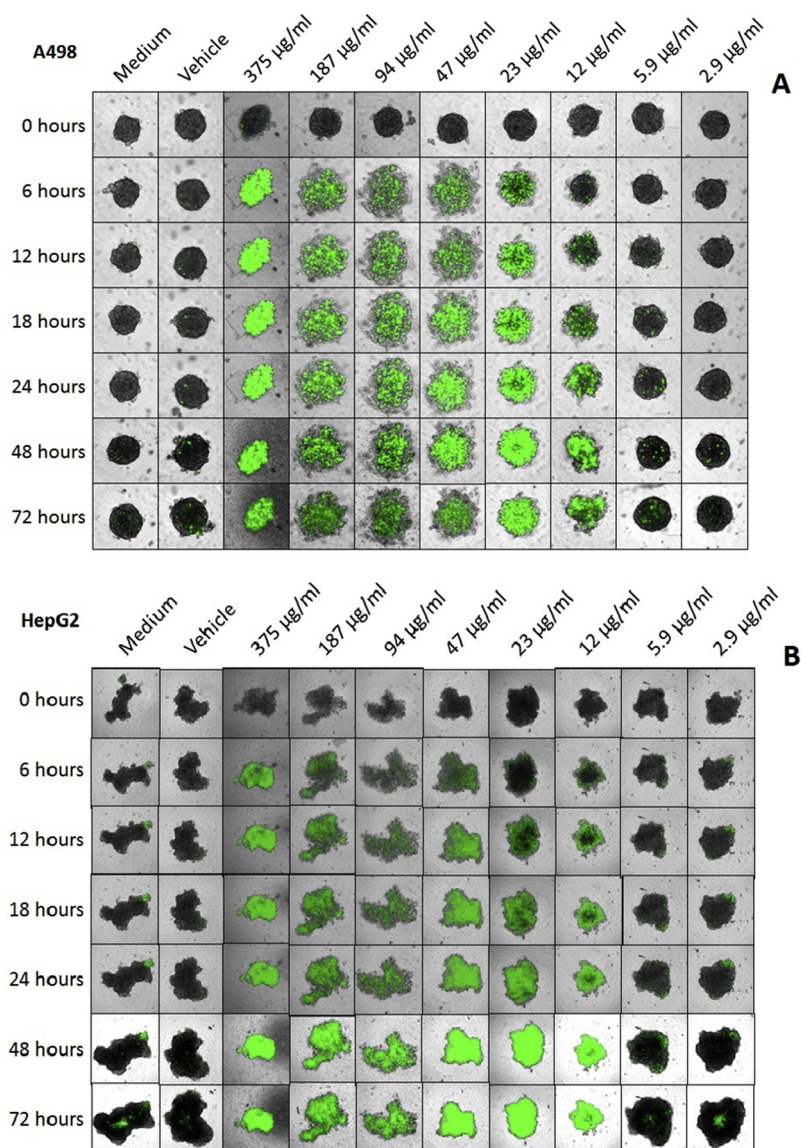


Fig. 4. Antitumor activity of PECA-NPs 5 against A498 (A) and HepG2 (B) tumor spheroids. The vehicle used was water.

forming carbanions, which then react with other monomers giving rise to polymer chains. The particle formation is a very complex mechanism that proceeds in three different steps. In the first step, oligomers are formed in the monomer droplet and the polymerization is ended at the oligomer stage by protons. Afterward, the oligomeric species aggregate to form NP nuclei and, in the final step, the nuclei interact with further monomers and oligomers to form the final NPs [42,43]. Several authors suggest that the molecular mass and the particle size of NPs are influenced by pH of the polymerization medium. The NP formation requires a pH below 3, indeed above this pH, due to the higher concentration of

OH⁻, the polymerization rate is very fast to obtain small particles [44,45]. Therefore, in order to have a controllable polymerization, an acidic solution is necessary [46].

In this work, a reproducible synthesis procedure for the preparation of PECA-NPs was developed. The NPs were prepared by emulsion polymerization of ECA using Tween 20. This surfactant is commonly used to stabilize numerous formulations [47,48] and the addition of a suitable concentration of Tween 20 to the polymerization medium is necessary for the stability of NP dispersion. During the polymerization reaction, in all the formulations prepared with a Tween 20

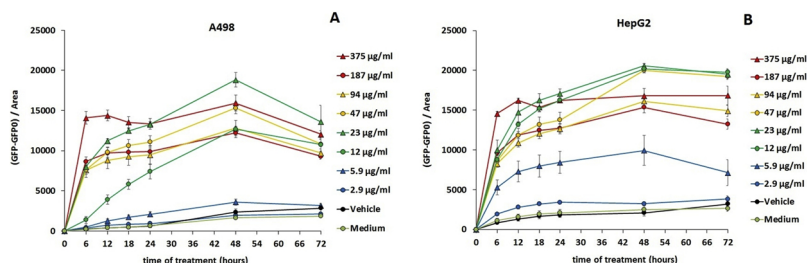


Fig. 5. Spheroid death at different times points in A498 (A) and HepG2 (B) tumor spheroids. The vehicle used was water.

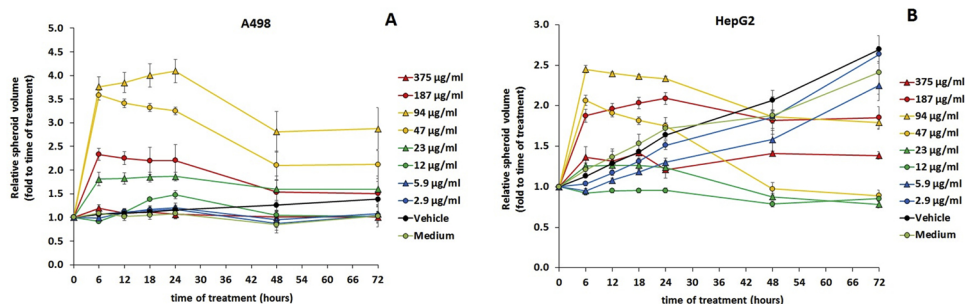


Fig. 6. Spheroid volume at different times points in A498(A) and HepG2 (B) tumor spheroids. The vehicle used was water.

concentration of 0.5% (w/v), visible aggregates are obtained, indicating reduced stability of these systems. Furthermore, it was observed that the increase of surfactant concentration to 1% (w/v) lead to a decrease in particle size and PDI values. ECA is very reactive, therefore if a high concentration is used, not all the monomer reacts to form the NPs and the excess can form polymeric strands and aggregates. As a result, purification procedure such as filtration [49] and repeated cycles of centrifugation [19] are needed. On the contrary, when the concentration of ECA is reduced, the rate of polymerization is very low.

The developed method allows the formation of spherical NPs, characterized by narrow colloidal size distribution. Particle size is an important parameter for drug delivery systems. It was reported that NPs with a particle size below 400 nm can go through vascular endothelium and accumulate at the cancer site; moreover, a capillary distribution and a uniform perfusion at the target site can be obtained with particles smaller than 1 μm [50]. The particle size of NPs (< 200 nm) is within the characteristic dimensional range of PECA-NPs obtained with the emulsion polymerization method, and it can be considered suitable for parenteral administration [51].

Concerning TEM observations, the ultrastructural morphology of PECA-NPs described as a spherical shape of nanosize particles may be a positive feature for particle internalization by cancer cells, as supposed in a paper related to the gold-NP of Chithrani et al. [52]. Therefore, the penetration of dark phosphotungstic acid inside PECA-NPs forming electron-dense granules can depend from the presence of hollow spaces in the internal structure of these NPs. In this way, anticancer drugs may be internalized inside PECA-NPs. Further, the surface negative electrical charge of NPs can also suggest a suitable device to bypass the immune system reaction *in vivo* and therefore considered useful for clinical applications [53]. Moreover, it has also been hypothesized that PECA-NPs may be able to overcome the multidrug resistance shown by tumor cells, allowing a specific transport mechanism associated with P-glycoprotein and the delivery of anticancer drugs only inside cancer cells, without any adverse interaction with cells of surrounding healthy tissues [54].

Dynamic light scattering analysis confirms that the particles are stable in terms of mean particle size and PDI during a period of 15 days, when stored in the dark at 25.0 $^{\circ}\text{C}$ or 4.0 $^{\circ}\text{C}$, therefore if the formulation is not used once prepared, it can be stored under these conditions for this time. On the contrary, a less stability of the NPs was observed in FBS, even if the size of these particles remains < 200 nm. FTIR and ^1H NMR results show the structure of PECA-NPs and the absence of non-polymerized monomer indicates that the polymerization is complete. The negative zeta potential may be due to the adsorption of anions [55] or scarce free carboxylic groups on the NPs surface [56].

Cytotoxicity of PECA-NPs against different cell lines has been previously reported. In our study, the PECA-NPs show dose-dependent cytotoxicity activity against Caco-2 cells. It is necessary to increase the NPs concentration from 7.5 to 75 $\mu\text{g}/\text{ml}$ to obtain a cell death of about 95%. This correlation between cytotoxicity and NPs concentration was observed previously by González-Martín et al. The authors prepared PECA-NPs and their toxicity against ATCC CCL-81 cell line was

evaluated. With NPs concentration of 789 $\mu\text{g}/\text{ml}$, cytotoxicity was found to be 100%, whereas when the concentration was decreased to 87.8 $\mu\text{g}/\text{ml}$ the toxicity was about 22% [57]. Conversely, in our work, NPs at concentrations of 75 $\mu\text{g}/\text{ml}$ exhibit high cytotoxicity. This discrepancy is probably due to the different cell line used. The toxic effect of PECA-NPs was also reported by Ibegbu et al., which proposed NPs of alkylglyceryl dextran and PECA. Cytotoxicity was assessed on bEnd3 cells and the experiments indicated that the NPs begin to exhibit toxic effects at concentrations of 25 $\mu\text{g}/\text{ml}$. The authors also prepared the NPs using another monomer, the butyl cyanoacrylate (PBCA-NPs) and, interestingly, it was found that PBCA-NPs were less toxic than PECA-NPs [58]. These results are in good agreement with those described in further research papers, in which, neither *in vitro* cytotoxicity was observed for PBCA-NPs [26,50,59]. The highest cytotoxicity of PECA-NPs is consistent with previous suggestions that the toxic effect of alkyl cyanoacrylate NPs is correlated with their velocity degradation (and therefore with the rate of release of degradation products) that is inversely proportional to the length of alkyl chain [20]. Brzoska et al. reported that, at the same concentration, NPs prepared with polyhexyl cyanoacrylate are less toxic than PBCA-NPs [60].

The mechanism of *in vitro* cytotoxicity for these NPs has not been properly clarified. Couvreur et al. [31] suggested that one of the most important degradation products is formaldehyde, which could cause cellular damage. In a recent work, it was reported the toxicity of intact NPs and NP degradation products in 12 different cell lines. Interestingly, it was observed that the cytotoxicity originated from intact NPs. Furthermore, the authors reported that the cytotoxicity was cell line dependent. This should be sought in the differences among cell lines in their capacity to interact and endocytose the NPs, and in the fact that tumor cell lines particularly are frequently characterized by altered pathways of cell signaling and apoptosis [61]. Further studies are needed to better understand the mechanism of alkyl cyanoacrylate NPs toxicity.

In this study, we evaluate the sensitivity of 2D cell cultures and 3D spheroid models to interaction of PECA-NPs using cytotoxicity as an endpoint. The traditional MTT assay on monolayer cell culture is not sufficient to evaluate the complex toxic effect of these NPs *in vivo* [62]. Recently, several research works reported the implication of tumor microenvironment in cancer growth, metastases development and resistance to anti-cancer therapies. 3D culture systems represent the predictive biological model of human condition mimicking tissue structure, signaling mechanisms and metabolism processes. In particular, 3D multicellular spheroid models have been demonstrated to be more representative of the tumor structure and microenvironment [63]. Using this model it can be determined the NP capability to enter leaky cancer vasculature by diffusion properties. Additionally, these models can help to better understand the probable NPs behavior *in vivo* before using animal models [64]. Therefore, the tumor spheroids as example of 3D cell cancer cultures have significant potential in the optimization of nano-chemotherapeutics and in determining their therapeutic abilities. The tested NPs exhibited a cytotoxic effect on both 3D tumor models, hepatocellular carcinoma and kidney adenocarcinoma, two of

the most commonly diagnosed cancers in the worldwide. Furthermore, it was observed that NPs concentration and treatment time influenced the antitumor activity of formulation. Comparing the results obtained with the MTT test on Caco-2 cell line in monolayer culture and cytotoxicity tested on human tumor spheroids we have similar results. In 3D spheroids we have the appearance of a marked cytotoxic effect for concentrations higher than 47 µg/ml; in 2D cell culture at a concentration of 75 µg/ml we have a cell death of about 95%. Some recent works report a greater sensitivity of the 3D models discovered as a cytotoxicity models [65], although others researches shows the two-dimensional cell cultures as a more sensitive system to different types of NPs. On the basis of these considerations, we used both experimental models to study NPs cytotoxicity and better predict the behavior of our *in vivo* formulations.

5. Conclusions

In this study, a simple and reproducible technique for the preparation of polymeric NPs endowed of anticancer activity was developed. The results demonstrate that the NPs obtained with this method are characterized by interesting tumor cytotoxicity against 3D spheroid models of hepatic and kidney cancer, offering an effective strategy to enhance anticancer therapy. Furthermore the concentration and the exposition time affect NP toxicity assessment. This work provides the basis for further research lines, because the entrapment of chemotherapeutic agents into these systems could result in a synergistic antitumor effect against cancer cells, both *in vitro* and *in vivo*. Additionally, theranostic NPs, which combine the functionality of both therapy and imaging, can be obtained loading these systems with diagnostic agents, such as indocyanine green [66]. In this way, the cancer is simultaneously treated and monitored. Compared to the standard monolayer cell cultures, the *in vitro* 3D tumor spheroid models increase the predictive outcome of cytotoxicity evaluation for NPs and represent rigorous tools to better characterize these platforms and for screening new drug delivery systems during the preclinical phase. The results obtained from the test with spheroids can be used to develop novel strategies for tumor treatment. However, tumor spheroids are simpler than *in vivo* models, hence the evaluation of pharmacokinetics and pharmacodynamics of NPs, such as the systemic interactions is not possible. For that reason, after utilizing the *in vitro* 3D spheroids to evaluate the antitumor activity of PECA-NPs, in the future, these promising agents should be tested *in vivo* in order to collect also such information.

Declaration of interest

The authors report no declarations of interest.

Funding

This research did not receive any specific grant from founding agencies in the public, commercial, or not-for-profit sector.

Acknowledgments

Authors wish to thank the team of the contract research organization Kitos Biotech s.r.l.s. for their technical and scientific support. We are grateful to Prof. Alberto Calligaro, whose relevant comments and technical suggestions for TEM analysis were an enormous help. We thank also to Dr. Massimo Boiocchi and Dr. Patrizia Vaghi for outstanding technical support.

Appendix A. Supplementary data

Supplementary material related to this article can be found, in the online version, at doi:<https://doi.org/10.1016/j.colsurfb.2019.02.036>.

References

- [1] C. Fitzmaurice, C. Allen, R.M. Barber, L. Barregard, Z.A. Bhutta, H. Brenner, T. Fleming, Global, regional, and national cancer incidence, mortality, years of life lost, years lived with disability, and disability-adjusted life-years for 32 cancer groups, 1990 to 2015: a systematic analysis for the global burden of disease study, *JAMA Oncol.* 3 (2017) 524–548.
- [2] G.V. Ratnam, K. Haritha, A.L. Rao, Drug targeting in neoplastic disorders, *Int. J. Res. Pharm. Chem.* 6 (2016) 623–630.
- [3] M. Ferrari, Cancer nanotechnology: opportunities and challenges, *Nat. Rev. Cancer* 5 (2005) 161.
- [4] T.G.G.M. Lammers, F. Kiessling, W.E. Hennink, G. Storm, Drug targeting to tumors: principles, pitfalls and (pre-) clinical progress, *J. Control. Release* 161 (2012) 175–187.
- [5] F. Danhier, O. Feron, V. Préat, To exploit the tumor microenvironment: passive and active tumor targeting of nanocarriers for anti-cancer drug delivery, *J. Control. Release* 148 (2010) 135–146.
- [6] H. Maeda, K. Tsukigawa, J. Fang, A retrospective 30 years after discovery of the enhanced permeability and retention effect of solid tumors: next-generation chemotherapeutics and photodynamic therapy-problems, solutions, and prospects, *Microcirculation* 23 (2016) 173–182.
- [7] T.G.G.M. Lammers, W.E. Hennink, G. Storm, Tumour-targeted nanomedicines: principles and practice, *Br. J. Cancer* 99 (2008) 392–397.
- [8] R.K. Jain, T. Stylianopoulos, Delivering nanomedicine to solid tumors, *Nat. Rev. Clin. Oncol.* 7 (2010) 653–664.
- [9] I. Brigger, C. Dubernet, P. Couvreur, Nanoparticles in cancer therapy and diagnosis, *Adv. Drug Deliv. Rev.* 54 (2002) 631–651.
- [10] C.M.J. Hu, S. Aryal, L. Zhang, Nanoparticle-assisted combination therapies for effective cancer treatment, *Ther. Deliv.* 1 (2010) 323–334.
- [11] L. Zhang, F.X. Gu, J.M. Chan, A.Z. Wang, R.S. Langer, O.C. Farokhzad, Nanoparticles in medicine: therapeutic applications and developments, *Clin. Pharmacol. Ther.* 83 (2008) 761–769.
- [12] S.R. Mudshinge, A.B. Deore, S. Patil, C.M. Bhalgat, Nanoparticles: emerging carriers for drug delivery, *Saudi Pharm. J.* 19 (2011) 129–141.
- [13] C. Pan, Y. Liu, M. Zhou, W. Wang, M. Shi, M. Xing, W. Liao, Theranostic pH-sensitive nanoparticles for highly efficient targeted delivery of doxorubicin for breast tumor treatment, *Int. J. Nanomed.* 13 (2018) 1119–1137.
- [14] P. Rychahou, Y. Bae, D. Reichel, Y.Y. Zaytseva, E.Y. Lee, D. Napier, H.L. Weiss, N. Roller, H. Frohmana, A. Le, B.M. Evers, Colorectal cancer lung metastasis treatment with polymer–drug nanoparticles, *J. Control. Release* 275 (2018) 85–91.
- [15] C.A. Quinto, P. Mohindra, S. Tong, G. Bao, Multifunctional superparamagnetic iron oxide nanoparticles for combined chemotherapy and hyperthermia cancer treatment, *Nanoscale* 7 (2015) 12728–12736.
- [16] E. Sulheim, H. Baghirov, E. Haartman, A. Bøe, A.K. Åslund, Y. Mørch, C. de Lange Davies, Cellular uptake and intracellular degradation of poly (alkyl cyanoacrylate) nanoparticles, *J. Nanobiotechnol.* 14 (2016) 1.
- [17] D. Katti, N. Krishnamurti, Anionic polymerization of alkyl cyanoacrylates: in vitro model studies for *in vivo* applications, *J. Appl. Polym. Sci.* 74 (1999) 336–344.
- [18] E. Fattal, M.T. Peracchia, P. Couvreur, Poly (alkylcyanoacrylates), in: A.J. Domb, J. Kost, D.M. Wiseman (Eds.), *Handbook of Biodegradable Polymers*, vol. 7, Harwood Academic Publisher, Amsterdam, 1998, Chapter 10.
- [19] J.L. Arias, V. Gallardo, S.A. Gomez-Lopera, R.C. Plaza, A.V. Delgado, Synthesis and characterization of poly (ethyl-2-cyanoacrylate) nanoparticles with a magnetic core, *J. Control. Release* 77 (2001) 309–321.
- [20] C. Lherm, R.H. Müller, F. Puisieux, P. Couvreur, Alkylcyanoacrylate drug carriers: II. Cytotoxicity of cyanoacrylate nanoparticles with different alkyl chain length, *Int. J. Pharm.* 84 (1992) 13–22.
- [21] C. Chauvierre, M.C. Marden, C. Vauthier, D. Labarre, P. Couvreur, L. Leclerc, Heparin coated poly (alkylcyanoacrylate) nanoparticles coupled to hemoglobin: a new oxygen carrier, *Biomaterials* 25 (2004) 3081–3086.
- [22] A. Čurić, J.P. Möschwitzer, G. Fricker, Development and characterization of novel highly-loaded itraconazole poly (butyl cyanoacrylate) polymeric nanoparticles, *Eur. J. Pharm. Biopharm.* 114 (2017) 175–185.
- [23] H. Baghirov, S. Melikishvili, Y. Mørch, E. Sulheim, A.K. Åslund, T. Hianik, C. de Lange Davies, The effect of poly (ethylene glycol) coating and monomer type on poly (alkyl cyanoacrylate) nanoparticle interactions with lipid monolayers and cells, *Colloids Surf. B: Biointerfaces* 150 (2017) 373–383.
- [24] C. Vauthier, C. Dubernet, E. Fattal, H. Pinto-Alphandary, P. Couvreur, Poly (alkylcyanoacrylates) as biodegradable materials for biomedical applications, *Adv. Drug Deliv. Rev.* 55 (2003) 519–548.
- [25] J.L. Arias, V. Gallardo, M.A. Ruiz, A.V. Delgado, Ftorafur loading and controlled release from poly (ethyl-2-cyanoacrylate) and poly (butylcyanoacrylate) nanoparticles, *Int. J. Pharm.* 337 (2007) 282–290.
- [26] L. Cabeza, R. Ortiz, J.L. Arias, J. Prados, M.A.R. Martínez, J.M. Entrena, R. Luque, C. Melguizo, Enhanced antitumor activity of doxorubicin in breast cancer through the use of poly (butylcyanoacrylate) nanoparticles, *Int. J. Nanomed.* 10 (2015) 1291–1306.
- [27] J.L. Arias, M.A. Ruiz, V. Gallardo, Á.V. Delgado, Tegafur loading and release properties of magnetite/poly (alkylcyanoacrylate) (core/shell) nanoparticles, *J. Control. Release* 125 (2008) 50–58.
- [28] M. Dubiak-Szepietowska, A. Karczmarczyk, M. Jönsson-Niedziółka, T. Winckler, K.H. Feller, Development of complex-shaped liver multicellular spheroids as a human-based model for nanoparticle toxicity assessment *in vitro*, *Toxicol. Appl. Pharmacol.* 294 (2016) 78–85.
- [29] H. Lei, S.C. Hofferberth, R. Liu, A. Colby, K.M. Tevis, P. Catalano, M.W. Grinstaff,

- Y.L. Colson, Paclitaxel-loaded expansile nanoparticles enhance chemotherapeutic drug delivery in mesothelioma 3-dimensional multicellular spheroids, *J. Thorac. Cardiovasc. Surg.* 149 (2015) 1417–1425.
- [30] G. Mehta, A.Y. Hsiao, M. Ingram, G.D. Luker, S. Takayama, Opportunities and challenges for use of tumor spheroids as models to test drug delivery and efficacy, *J. Control. Release* 164 (2012) 192–204.
- [31] P. Couvreur, V. Lenaerts, D. Leyh, P. Guiot, M. Roland, Design of biodegradable polyalkylcyanoacrylate nanoparticles as a drug carrier, in: S.S. Davis, L. Illum, J.G. McVie, E. Tomillson (Eds.), *Microspheres and Drug Therapy: Pharmaceutical Immunological and Medical Aspects*, Elsevier Science, Amsterdam, 1984 Chapter 3.
- [32] P. Couvreur, C. Vauthier, Polyalkylcyanoacrylate nanoparticles as drug carrier: present state and perspectives, *J. Control. Release* 17 (1991) 187–198.
- [33] M. Locke, N. Kirhman, Preparation procedures for examining icosahedral and filamentous viruses, *J. Ultrastruct. Res.* 47 (1971).
- [34] C.A. Schneider, W.S. Rasband, K.W. Eliceiri, NIH Image to ImageJ: 25 years of image analysis, *Nat. Methods* 9 (2012) 671–675.
- [35] M. Selby, R. Delosh, J. Laudeman, C. Ogle, R. Reinhart, T. Silvers, S. Lawrence, R. Kinders, R. Parchment, B.A. Teicher, D.M. Evans, 3D models of the NCI60 cell lines for screening oncology compounds, *SLAS Discov.* 22 (2017) 473–483.
- [36] F.P. Fiorentino, L. Bagella, I. Marchesi, A new parameter of growth inhibition for cell proliferation assays, *J. Cell. Physiol.* 233 (2018) 4106–4115.
- [37] M. Vinci, S. Gowan, F. Boxall, L. Patterson, M. Zimmermann, W. Court, C. Lomas, M. Mendiola, D. Hardisson, S.A. Eccles, Advances in establishment and analysis of three-dimensional tumor spheroid-based functional assays for target validation and drug evaluation, *BMC Biol.* 10 (2012).
- [38] T. Matsubayashi, M. Tenjimbayashi, K. Manabe, K.-H. Kyung, B. Ding, S. Shiratori, A facile method of synthesizing size-controlled hollow cyanoacrylate nanoparticles for transparent superhydrophobic/oleophobic surface, *RSC Adv.* 6 (2016) 15877–15883.
- [39] A. Lankoff, W.J. Sandberg, A. Wegierek-Ciuk, H. Lisowska, M. Refsnæs, B. Sartowska, P.E. Schwarzec, S. Meczynska-Wielgosza, M. Wojewodzkaa, M. Kruszewska, The effect of agglomeration state of silver and titanium dioxide nanoparticles on cellular response of HepG2, A549 and THP-1 cells, *Toxicol. Lett.* 208 (2012) 197–213.
- [40] N. Behan, C. Birkinshaw, N. Clarke, Poly n-butyl cyanoacrylate nanoparticles: a mechanistic study of polymerisation and particle formation, *Biomaterials* 22 (2001) 1335–1344.
- [41] J. Nicolas, P. Couvreur, Synthesis of poly (alkyl cyanoacrylate)-based colloidal nanomedicines, *Wiley Interdiscip. Rev. Nanomed. Nanobiotechnol.* (2009) 111–127.
- [42] G. Yordanov, Poly (alkyl cyanoacrylate) nanoparticles as drug carriers: 33 years later, *Bulg. J. Chem.* 1 (2012) 61–72.
- [43] G. Yordanov, R. Skrobanska, A. Evangelatov, Colloidal formulations of etoposide based on poly (butyl cyanoacrylate) nanoparticles: preparation, physicochemical properties and cytotoxicity, *Colloid. Surf. B: Biointerfaces* 101 (2013) 215–222.
- [44] K.S. Soppimath, T.M. Aminabhavi, A.R. Kulkarni, W.E. Rudzinski, Biodegradable polymeric nanoparticles as drug delivery devices, *J. Control. Release* 70 (2001) 1–20.
- [45] S.C. Yang, H.X. Ge, Y. Hu, X.Q. Jiang, C.Z. Yang, Formation of positively charged poly (butyl cyanoacrylate) nanoparticles stabilized with chitosan, *Colloid Polym. Sci.* 278 (2000) 285–292.
- [46] G. Yordanov, Z. Bedzhova, Poly (ethyl cyanoacrylate) colloidal particles tagged with Rhodamine 6G: preparation and physicochemical characterization, *Cent. Eur. J. Chem.* 9 (2011) 1062.
- [47] N.C. Christov, D.N. Ganchev, N.D. Vassileva, N.D. Denkov, K.D. Danov, P.A. Kralchevsky, Capillary mechanisms in membrane emulsification: oil-in-water emulsions stabilized by Tween 20 and milk proteins, *Colloids Surf. A: Physicochem. Eng. Aspects* 209 (2002) 83–104.
- [48] Z. Zhang, J. Zhang, C. Qu, D. Pan, Z. Chen, L. Chen, Label free colorimetric sensing of thiocyanate based on inducing aggregation of Tween 20-stabilized gold nanoparticles, *Analyst* 137 (2012) 2682–2686.
- [49] M.T. Peracchia, C. Vauthier, F. Puisieux, P. Couvreur, Development of sterically stabilized poly (isobutyl 2-cyanoacrylate) nanoparticles by chemical coupling of poly (ethylene glycol), *J. Biomed. Mater. Res.* 34 (1997) 317–326.
- [50] J. Duan, Y. Zhang, S. Han, Y. Chen, B. Li, M. Liao, W. Chen, X. Deng, J. Zhao, B. Huang, Synthesis and in vitro/in vivo anti-cancer evaluation of curcumin-loaded chitosan/poly (butyl cyanoacrylate) nanoparticles, *Int. J. Pharm.* 400 (2010) 211–220.
- [51] T. Musumeci, C.A. Ventura, I. Giannone, B. Ruozi, L. Montenegro, R. Pignatello, G. Puglisi, PLA/PLGA nanoparticles for sustained release of docetaxel, *Int. J. Pharm.* 325 (2006) 172–179.
- [52] B.D. Chithrani, A.A. Ghazani, W.C. Chan, Determining the size and shape dependence of gold nanoparticle uptake into mammalian cells, *Nano Lett.* 6 (2006) 662–668.
- [53] C. He, Y. Hu, L. Yin, C. Tang, C. Yin, Effects of particle size and surface charge on cellular uptake and biodistribution of polymeric nanoparticles, *Biomaterials* 31 (2010) 3657–3666.
- [54] C. Melguizo, L. Cabeza, J. Prado, R. Ortiz, O. Caba, A.R. Rama, A.V. Delgado, J.L. Arias, Enhanced antitumoral activity of doxorubicin against lung cancer cells using biodegradable poly(butylcyanoacrylate) nanoparticles, *Drug Des. Dev. Ther.* 9 (2015) 6433–6444.
- [55] S.J. Douglas, L. Illum, S.S. Davis, J. Krueger, Particle size and size distribution of poly (butyl-2-cyanoacrylate) nanoparticles: I. Influence of physicochemical factors, *J. Colloid Interface Sci.* 101 (1984) 149–158.
- [56] J.L. Arias, V. Gallardo, M.A. Ruiz, Á.V. Delgado, Magnetite/poly (alkylcyanoacrylate)(core/shell) nanoparticles as 5-fluorouracil delivery systems for active targeting, *Eur. J. Pharm. Biopharm.* 69 (2008) 54–63.
- [57] G. González-Martín, C. Figueroa, I. Merino, A. Osuna, Allopurinol encapsulated in polycyanoacrylate nanoparticles as potential lysosomotropic carrier: preparation and trypanocidal activity, *Eur. J. Pharm. Biopharm.* 49 (2000) 137–142.
- [58] D.M. Ibegbu, A. Boussahel, S.M. Cragg, J. Tsibouklis, E. Barbu, Nanoparticles of alkylglyceryl dextran and poly (ethyl cyanoacrylate) for applications in drug delivery: preparation and characterization, *Int. J. Polym. Mater. Polym. Biomater.* 66 (2017) 265–279.
- [59] X. Jin, S. Asghar, X. Zhu, Z. Chen, C. Tian, L. Yin, Q. Ping, Y. Xiao, In vitro and in vivo evaluation of 10-hydroxycamptothecin-loaded poly (n-butyl cyanoacrylate) nanoparticles prepared by miniemulsion polymerization, *Colloids Surf. B* 162 (2018) 25–34.
- [60] M. Brzoska, K. Langer, C. Coester, S. Loitsch, T.O.F. Wagner, C.V. Mallinckrodt, Incorporation of biodegradable nanoparticles into human airway epithelium cells—in vitro study of the suitability as a vehicle for drug or gene delivery in pulmonary diseases, *Biochem. Biophys. Res. Commun.* 318 (2004) 562–570.
- [61] E. Sulheim, T.G. Iversen, V. To Nakstad, G. Klinkenberg, H. Sletta, R. Schmid, A.R. Hatletveit, A.M. Wågbo, A. Sundan, T. Skotland, K. Sandvig, Y. Mørch, Cytotoxicity of poly (Alkyl cyanoacrylate) nanoparticles, *Int. J. Mol. Sci.* 18 (2017) 2454.
- [62] A.S. Mikhail, S. Eetezadi, C. Allen, Multicellular tumor spheroids for evaluation of cytotoxicity and tumor growth inhibitory effects of nanomedicines in vitro: a comparison of docetaxel-loaded block copolymer micelles and Taxotere®, *PLoS One* 8 (2013) e62630.
- [63] E.C. Costa, A.F. Moreira, D. de Melo-Diogo, V.M. Gaspar, M.P. Carvalho, I.J. Correia, 3D tumor spheroids: an overview on the tools and techniques used for their analysis, *Biotechnol. Adv.* 34 (2016) 1427–1441.
- [64] D.N. Ho, N. Kohler, A. Sigdel, R. Kalluri, J.R. Morgan, C. Xu, S. Sun, Penetration of endothelial cell coated multicellular tumor spheroids by iron oxide nanoparticles, *Theranostics* 2 (2012) 66.
- [65] C.C. Bell, A.C.A. Dankers, V.M. Lauschke, R. Sison-Young, R. Jenkins, C. Rowe, C.E. Goldring, K. Park, S.L. Regan, T. Walker, C. Schofield, A. Baze, A.J. Foster, D.P. Williams, A.W.M. van de Ven, F. Jacobs, J.V. Houdt, T. Lähteenmäki, J. Snoeys, S. Juhila, L. Richert, M. Ingelman-Sundberg, Comparison of hepatic 2D sandwich cultures and 3D spheroids for long-term toxicity applications: a multicenter study, *Toxicol. Sci.* 162 (2018) 655–666.
- [66] E.P. Porcu, A. Salis, E. Gavini, G. Rassa, M. Maestri, P. Giunchedi, Indocyanine green delivery systems for tumour detection and treatments, *Biotechnol. Adv.* 34 (2016) 768–789.